Published in Applied Physics B: Lasers and Optics 90, issue 2, 187-190, 2008
which should be used for any reference to this wor

Applications for quantum cascade lasers and detectors in mid-infrared high-resolution heterodyne astronomy

P. KRÖTZ[1,✉], D. STUPAR[1], J. KRIEG[1], G. SONNABEND[1], M. SORNIG[1], F. GIORGETTA[2], E. BAUMANN[2], M. GIOVANNINI[2], N. HOYLER[2], D. HOFSTETTER[2], R. SCHIEDER[1]

[1] I. Physikalisches Institut, Universität zu Köln, Zülpicher Str. 77, 50937 Köln, Germany
[2] University of Neuchatel, 1 A.-L. Breguet, Neuchatel 2000, Switzerland

ABSTRACT Quantum cascade (QC) structures, for both emitting and detecting mid-infrared radiation, are powerful devices for spectroscopy. QC lasers (QCLs), which have been built for nearly 15 years, already play the leading role in certain wavelength regions. QC detectors (QCDs) are a fairly new development, which has been evolving from the QCL research. In high-resolution heterodyne spectrometers for astronomy, such as the Cologne tuneable heterodyne infrared spectrometer (THIS), QC devices help to open new windows to space as discussed in this paper. We will briefly review the use of QC devices in THIS, show recent results in measuring planetary atmospheric dynamics and give an outlook to astronomical goals for the future.

PACS 33.70.Jg

1 Introduction

High-resolution ($R > 10^6$) spectroscopy with THIS (tuneable heterodyne infrared spectrometer) [1–3] provides data of fully resolved molecular lines in the mid infrared. In this wavelength region many molecules, especially those without permanent dipole moment (and thus not observable at radio wavelengths), can be studied. The high resolution allows us to peek through narrow atmospheric windows. It is then possible to deduce physical parameters of planetary trace gases, dynamics in circumstellar envelopes, planetary atmospheres [3], solar features [4], the interstellar medium, etc. The basic principle is to superimpose the signals from the observed astronomical object and the local oscillator (LO), which yields an easy to analyse intermediate frequency in the radio region, still including all spectroscopic information of the source. Currently the instrument uses quantum cascade lasers (QCLs) as LO and a mercury–cadmium-telluride (MCT) detector. Quantum cascade detectors (QCDs) and quantum well infrared photodetectors (QWIPs) are under investigation to extend the spectral coverage towards longer wavelengths.

✉ Fax: +49-221-470-5162, E-mail: kroetz@ph1.uni-koeln.de

2 Instrumentation

Depending on the availability of QCLs the spectrometer is designed for 7–17 μm. Superpositioning of signal and LO is done with a confocal Fabry–Pérot diplexer (see Fig. 1) enhancing the signal-combining efficiency compared to a beam splitter. 60% transmission of the LO signal at the diplexer resonance can be combined to > 95% reflection of the sky signal between the diplexer resonances, whereas with a beam splitter the two values cannot add up to more than 100%. The diplexer also acts as a frequency stabiliser, suppresses incoherent laser emission and minimises the optical feedback to the LO. For calibration purposes the signal can be rapidly switched by a fast scanner mirror from the source to a reference position in the sky, to two calibration loads within the spectrometer and to a reference gas cell. Frequency stability is provided by a commercial stabilised He–Ne laser which the diplexer is locked to. The mixing is performed by a broadband MCT detector, and the frequency analysis by an in-house-built acousto-optical spectrometer (AOS) with an instantaneous bandwidth of 3 GHz and an intrinsic resolution bandwidth of 1 MHz. The spectrometer is easily transportable and adaptable to virtually any telescope. For detailed information about THIS, see [1].

3 Quantum cascade lasers as local oscillators

Quantum cascade lasers [5] are the perfect oscillators for infrared heterodyne spectroscopy. Line widths have been measured to be smaller than the intrinsic resolution bandwidth of the AOS of 1 MHz [3]. Better than lead-salt diodes, they provide enough optical laser power of 10 to some 100 mW, and can be grown for virtually any desired infrared wavelength. Therefore, they overcome the limitations of conventional mid-infrared heterodyne systems [6], which are confined to a few transition frequencies of the gas laser used (mostly CO_2). So far, only QCLs with distributed feedback (DFB, Fig. 2) were used. Those devices are single-mode lasers and can be temperature tuned only over a limited range of a few cm^{-1}. Soon, an external-cavity setup will provide ‘real’ tuneability over many wavenumbers (see below).

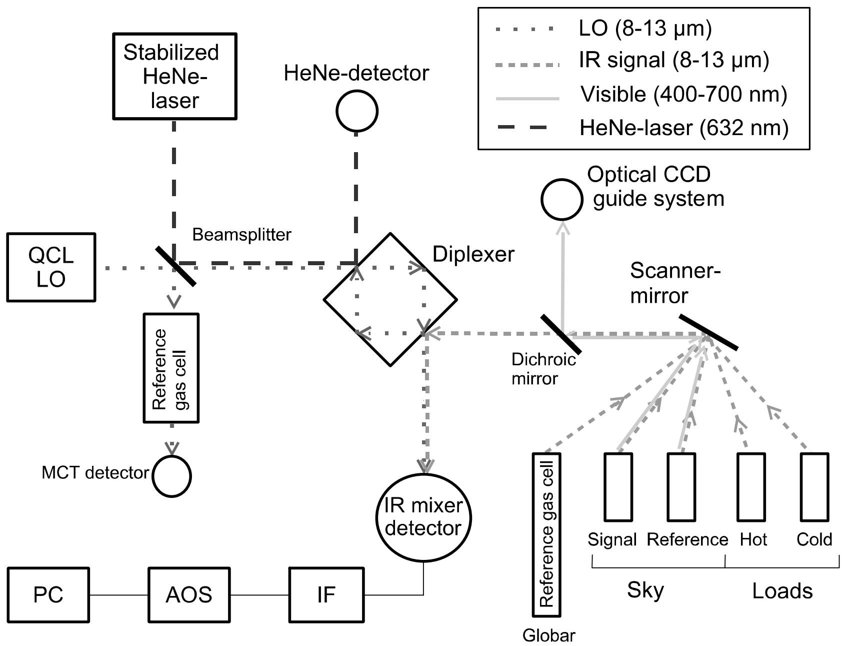

FIGURE 1 Schematic of the spectrometer THIS

4 QCL with external cavity

Combining Fabry–Pérot QCLs (FP–QCLs) with an external cavity (EC) for wavelength control yields a tuneable, broadband laser source which can be used to measure molecular lines over a range of up to 250 cm^{-1} [7]. This technique is another breakthrough for the application of QCLs in THIS as it could provide full wavelength coverage in the mid infrared with only a handful of local oscillators. Such a system will enable easy and economical investigations of many different molecular lines. We are currently integrating an EC setup in our spectrometer THIS, and first tests are promising [8]. Figure 2 shows the setup scheme of the EC in Littrow configuration, which provides full coverage over a range of 30 cm^{-1} when using our FP–QCL around 1130 cm^{-1}. Figure 3 shows a SO_2 spectrum near 1146 cm^{-1} measured with the laboratory setup. A single frequency can be tuned mode-hop-free over 0.28 cm^{-1} by coordinated change of drive current and resonator length. The lower part of Fig. 3 shows an internally coupled Fabry–Pérot interferometer (icFPI [9]) spectrum that demonstrates the ability of continuous tuning of the laser frequency. The experimental results demonstrate that coupling of QCL and EC is sufficient to cover any desired wavelength within the range of a FP–QCL for astronomical observation purposes. The QCL used in this experiment was kindly provided by C. Sirtori, Université Paris VII.

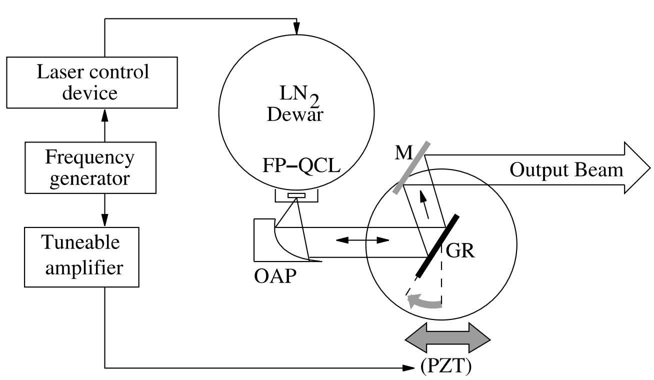

FIGURE 2 External-cavity setup

5 Quantum cascade detectors

Quantum cascade structures can also be used as detectors, which are then called quantum cascade detectors (QCDs). In contrast to the photoconductive QWIPs, which involve a bound to quasibound optical transition, the QCD is based on a bound to bound transition, whose excited state is resonantly coupled to an extraction cascade (phonon stair) transporting electrons vertically to the ground state of the next spatial period of the quantum cascade. As the QCD operates in a photovoltaic mode, no bias has to be applied, resulting in zero dark current and consequently no dark-current

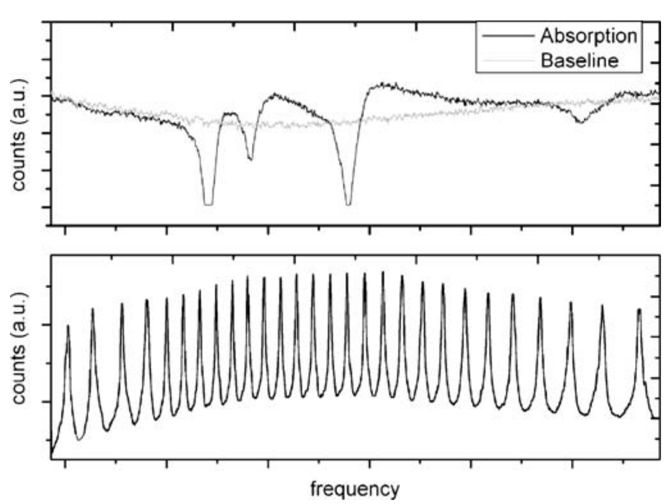

FIGURE 3 SO_2 spectrum near 1136 cm^{-1} measured with EC–QCL and icFPI fringes (FSR = 300 MHz) of the EC–QCL by tuning the laser

noise. QCDs have been demonstrated first for THz frequencies [10], and are now available in three different material systems (GaAs/AlGaAs, InGaAs/InAlAs and InGaAs/AlAsSb) covering a large wavelength range between 2.2 and 84 μm. First tests [11] were done with a device operating at 16.5 μm and using miniband-based vertical transport. This concept allowed the construction of a longitudinal optical phonon extraction stair with two rungs without abandoning the necessary high device resistance. At 10 K, we observed a responsivity of 1.72 mA/W and a Johnson noise limited detectivity of $2.2 \times 10^9\ \mathrm{cm}\sqrt{\mathrm{Hz}}/\mathrm{W}$. Altogether, this design resulted in detection at temperatures of up to 90 K. Based on the similar detection mechanisms of QCDs and QWIPs, and extrapolating our high-frequency results with a 5.3-μm QCD [12], we do not expect that an optimised QCD will have a slower response than a QWIP. Although QCDs lack an intrinsic gain mechanism resulting typically in low responsivities on the order of some mA/W, their superior high-frequency and noise properties compared to standard MCT detectors make them very interesting for applications in infrared astronomy. An improved design utilising a higher-lying miniband, optimised barrier thicknesses and some fine tuning in the active well thickness has led to a better temperature behaviour of the device, especially in terms of signal-to-noise ratio, and an increased low-temperature responsivity of 4.5 mA/W, as shown in Fig. 4. At 95 K, the responsivity was still 3.8 mA/W, whereas the first design resulted in 0.7 mA/W at 90 K. Further development in this direction together with the absence of dark-current noise is expected to lead to a decisive advantage of QCDs compared to MCTs, which will fully justify their implementation into THIS.

6 Applications: planetary wind measurements

The field of planetary atmospheres, and especially the Martian atmosphere, experienced a boost in the past decade because of many space missions including orbiters and landers. Data from these missions evolved into detailed atmospheric circulation models [13]. One crucial parameter of such models is zonal wind. However, for accurate wind measurements ($\delta v \approx 10\ \mathrm{m/s}$), satellite instruments are not yet adequate. Infrared heterodyne spectroscopy can provide the needed high spectral resolution and also has, in contrast to radio observations, the advantage of a small field of view, which allows mapping on the planetary disc with reasonably good spatial resolution, even with moderately sized telescopes. With THIS, Martian winds at altitudes around 70 km could be measured and mapped with an accuracy of $\delta \upsilon \approx 1\ \mathrm{MHz}$ (i.e. $\delta v \approx 10\ \mathrm{m/s}$). Zonal wind velocities were retrieved by measuring the Doppler shift between CO_2 absorption near the ground level and high-altitude non-local thermodynamical equilibrium (LTE) CO_2 emission (Fig. 5: plotted resolution: 1 MHz, integration time: 1.5 h). Compared to model predictions of the Mars Climate Database our measurements, done at the McMath Pierce Solar Telescope at Kitt Peak, USA, show a nice agreement [14], and further observations are planned for 2007/8 to cover more of the Martian year. Non-LTE emission is also evident in the atmosphere of Venus, which enabled wind observations within a coordinated ground-based observing campaign in support of European Space Agency's (ESA) orbiter Venus Express in May/June 2007.

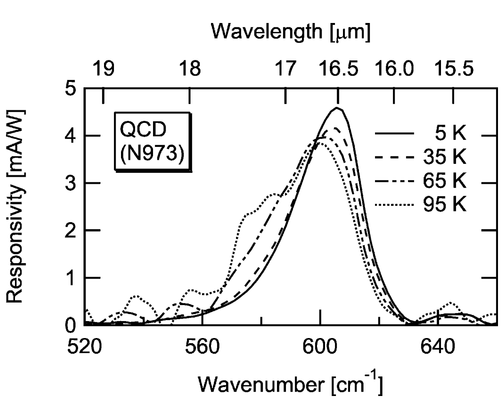

FIGURE 4 QCD responsivity for different temperatures

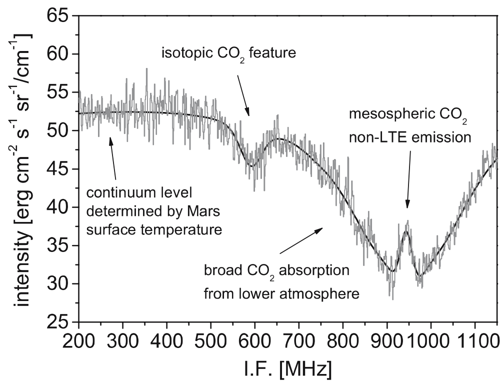

FIGURE 5 Spectrum of the CO_2 feature at 959.4 cm^{-1} on Mars, measured with THIS

7 Future plans

There are many possible applications for a high-resolution spectrometer like THIS in astrophysics: on Mars, for example, observations of methane (e.g. as claimed in [15]) could suggest either biotic or volcanic activity, both of which are thought to be not present today. Also, targets outside the solar system would be possible: detailed observations of carbohydrates in stellar atmospheres would test models of the chemical evolution of the universe; proto-stellar and proto-planetary discs could provide new hints on star formation and extra-solar planets. In the following, two projects which are currently ongoing will be introduced.

7.1 SO_2 *on Io*

An intriguing object for future investigations is Jupiter's moon Io. Its orbit within Jupiter's plasma torus, its high volcanic activity and its tenuous atmosphere make it a target of high scientific interest. A variety of questions need to be answered, one being perfectly suited for THIS: the interconnection of Io's atmosphere with Jupiter. A study of the dynamical properties of the atmosphere by observing SO_2 molecular features around 8.7-μm wavelength by high-resolution spectroscopy from the ground in combination with new theoretical approaches will lead to an improved understanding of the origin and the characteristics of the atmosphere and how it is affected by the plasma environment of Jupiter. Most observations nowadays confirm a picture of Io's atmosphere that is composed of a thick localised 'spotty' atmosphere produced by Io's strong volcanic activity and a more homogeneous and extended atmosphere produced by sublimation of SO_2 frost from Io's surface. The relative importance of both processes, however, is still not clear. Estimates of the average column density of Io's SO_2 atmosphere range from 5×10^{15} to $1 \times 10^{17}\,\mathrm{cm}^{-2}$ [16]. Models for Io's atmospheric temperature profile predict a steep temperature increase from around 120 K near Io's surface to up to 1500 K in the thermosphere [17]. Despite much progress in understanding Io's atmosphere over the last 30 years, it is still very poorly constrained. First model calculations for SO_2 detection on Jupiter's moon Io are available and first observations are planned for 2008.

7.2 *Cold molecular hydrogen in the interstellar medium*

Observing cold (≈ 10 K) molecular hydrogen is a very difficult task. Excitation energies of the lowest transitions (at 17.04 and 28.22 μm) are high (> 500 K), so no emission can be seen. Nearly all information on the distribution of H_2 in space is deduced from abundances of tracer molecules like CO. To check this assumptive procedure, we want to measure the H_2 abundance directly at 17 μm and later at 28 μm by observing the absorption against warm background sources. Comparing with CO data then yields a new determination of the CO/H_2 ratio. It will also be interesting to investigate the dynamics and abundance of molecular hydrogen in proto-stellar discs or in the atmospheres of the giant planets Jupiter, Saturn, Uranus and Neptune. THIS is also proposed as a second-generation instrument on SOFIA, the Stratospheric Observatory For Infrared Astronomy, scheduled to perform its first test flights in 2008. From 13-km altitude, this modified Boeing 747 equipped with a 2.5-m mirror will provide a clear window through the atmosphere, avoiding 99% of the telluric water vapour. This is essential for the planned measurements at 28 μm.

ACKNOWLEDGEMENTS The authors gratefully acknowledge Carlo Sirtori (University of Paris, Thales) for providing the FP–QCL, and financial support from DFG special grant 494 and the Professorship Program of the Swiss National Science Foundation.

REFERENCES

1 G. Sonnabend, M. Sornig, P. Krötz, D. Stupar, R. Schieder, submitted to J. Quant. Spectrosc. Radiat. Transfer (2007)
2 D. Wirtz, G. Sonnabend, R. Schieder, Spectrochim. Acta A **58**, 2457 (2002)
3 G. Sonnabend, D. Wirtz, R. Schieder, Appl. Opt. **44**, 7170 (2005)
4 G. Sonnabend, D. Wirtz, R. Schieder, P.F. Bernath, Appl. Opt. **233**, 205 (2006)
5 J. Faist, F. Capasso, D.L. Sivco, C. Sirtori, A.L. Hutchinson, A.Y. Cho, Science **264**, 553 (1994)
6 T. Kostiuk, K.E. Fast, T.A. Livengood, T. Hewagama, J.J. Goldstein, F. Espenak, D. Buhl, Geophys. Res. Lett. **28**, 2361 (2001)
7 R. Maulini, A. Mohan, M. Giovannini, J. Faist, E. Gini, Appl. Phys. Lett. **88**, 201 113 (2006)
8 D. Stupar, J. Krieg, P. Krötz, M. Sornig, G. Sonnabend, T. Giesen, R. Schieder, submitted to Appl. Opt. (2007)
9 M. Reich, R. Schieder, H.J. Clar, G. Winnewisser, Appl. Opt. **25**, 130 (1986)
10 M. Graf, G. Scalari, D. Hofstetter, J. Faist, H. Beere, E. Linfield, D. Ritchie, G. Davies, Appl. Phys. Lett. **84**, 475 (2004)
11 F.R. Giorgetta, E. Baumann, M. Graf, L. Ajili, N. Hoyler, M. Giovannini, J. Faist, G. Sonnabend, P. Krötz, D. Hofstetter, Appl. Phys. Lett. **90**, 231 111 (2007)
12 D. Hofstetter, M. Graf, T. Aellen, J. Faist, L. Hvozdara, S. Blaser, Appl. Phys. Lett. **89**, 1119 (2006)
13 S.R. Lewis, M. Collins, P.L. Read, F. Forget, F. Hourdin, R. Fournier, C. Hourdin, O. Talagrand, J.-P. Huot, J. Geophys. Res. **104**, 24 177 (1999)
14 G. Sonnabend, M. Sornig, P. Krötz, R. Schieder, K.E. Fast, Geophys. Res. Lett. **33**, 18 201 (2006)
15 V.A. Krasnopolsky, G.L. Bjoraker, M.J. Mumma, D.E. Jennings, J. Geophys. Res. **102**, 6525 (1997)
16 G.E. Ballester, M.A. McGrath, D.F. Stobel, X. Zhu, P.D. Feldman, H.W. Moos, Icarus **111**, 2 (1994)
17 P. Sartoretti, M.A. McGrath, F. Paresce, Icarus **108**, 272 (1994)